

# Dynamical purification phase transition induced by quantum measurements

Michael J. Gullans and David A. Huse

*Department of Physics, Princeton University, Princeton, New Jersey 08544, USA*

(Dated: April 22, 2022)

Continuously monitoring the environment of an open quantum many-body system reduces the entropy of (purifies) the reduced density matrix of the system, conditional on the outcome of the measurements. We show that a balanced competition between measurements and entangling interactions within the system can result in a dynamical purification phase transition between (i) a phase that locally purifies at a constant rate, and (ii) a phase where the purification time diverges exponentially in the system size. We establish our results by studying a class of random quantum circuits with measurements that are examples of Clifford circuits, which allows numerical finite-size studies of this phase transition for hundreds of qubits. This phase transition for mixed initial states occurs concurrently with a recently identified entanglement phase transition in this model for pure initial states; thus, our work provides additional insight into this novel class of entanglement phase transitions. Unlike for pure initial states, the mutual information of an initially completely-mixed state grows at most logarithmically in time, which should allow improved numerical studies of the transition in non-Clifford models, using matrix product methods. The purification dynamics studied here should also be more robust in experiments, where imperfections generically reduce entanglement and drive the system towards mixed states.

*Introduction.*—In thermodynamic equilibrium, pure quantum states can only be achieved at absolute zero temperature. The nonequilibrium thermodynamic cost of purification is encoded in the third law of thermodynamics, which states that it is impossible to reach a zero entropy (pure) quantum state in a finite amount of time. In quantum information science, purification plays an essential role in many models of quantum computation, where one often assumes access to highly pure computational or ancilla qubits [1]. Although it is known that the requisite purification is possible given sufficiently fine control over a quantum system and its environment [2–5], the question of whether a generic interacting many-body quantum system coupled to a finite temperature bath (i.e., an open quantum system) can be driven to a pure state remains less understood [6, 7].

An essential resource in controlling open quantum systems is the ability to make measurements of the system, which can then be used to perform feedback and conditional control (e.g., the famous Maxwell demon) [8]. Purification, however, does not require any feedback because the continuous monitoring of the environment can be used to continually gain information about the system; thereby, reducing the number of accessible states consistent with the measurement record and the intermediate dynamics [9–11]. Naively, one expects that continuous, perfect monitoring will rapidly purify the system; however, it is known from the study of quantum error correcting codes that quantum states can be protected from extensive numbers of local measurements [12–14]. Recently, there has been significant experimental progress towards realizing the requisite ingredients for such measurement-driven purification of many-body states in quantum computing platforms [15–24].

In this paper, we show that there is a dynamical purification phase transition as one changes the measure-

ment rate in a class of random quantum circuit models with measurements. For pure initial states, it was shown recently that there is an entanglement phase transition in these models from area-law to volume-law entanglement [25–28]. We show that, for completely-mixed initial states, this entanglement phase transition transforms into a dynamical purification transition between a “pure” phase, with a constant purification rate in the thermodynamic limit, and a “mixed” phase, where the purification time diverges exponentially in system size. Thus, if one takes the simultaneous limit of an infinite system and infinite time, with any power-law relation between system size and time, then an initially mixed state has a nonzero long-time entropy density in the mixed phase, while it becomes pure in the pure phase.

A crucial distinction for mixed initial states is that the late-time bipartite mutual information grows at most logarithmically in time, instead of the rapid linear-in-time growth seen for pure initial states. This slow growth of entanglement can be interpreted as a type of natural protection of part of the Hilbert space against measurement induced decoherence, which bolsters the connection between these transitions and quantum error correcting codes [29]. Furthermore, representing the mixed state using matrix product methods should allow access to much larger system sizes in numerics than for pure initial states. Finally, these results also have positive implications for the experimental study of this novel class of phase transitions, where imperfections generically reduce entanglement and drive the system towards mixed states.

The entanglement phase transition has now been shown to appear quite generically in models whenever there is a balanced competition between unitary dynamics that grows entanglement of the system and a measurement or decoherence process that reduces the en-

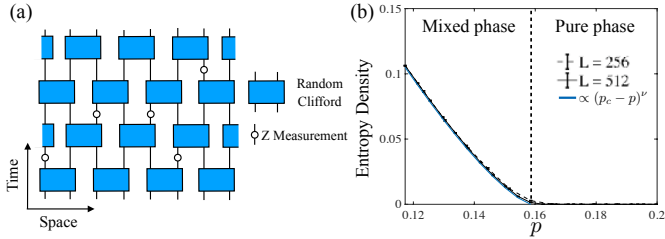


FIG. 1. (a) Random hybrid quantum circuit model studied in this work. Local two-qubit unitaries are drawn uniformly from the Clifford group in a 1D brickwork arrangement with periodic boundary conditions. These gates are interspersed by projective  $Z$  measurements with probability  $p$  at each site. (b) Phase diagram for the late-time, average entropy density  $\langle S(\rho) \rangle / L$  starting from the completely-mixed initial state. We took time  $t = 4L$  and  $L = 256$  and  $512$  to limit finite-size effects, although signatures of the transition appear already at  $L = 8$ . Blue curve shows  $\sim (p_c - p)^\nu$  for  $p \leq p_c = 0.1585(5)$  and  $\nu = 1.32(5)$  obtained below.

tanglement. To establish the connection to purification transitions we, therefore, study the model introduced in Ref. [28] [see Fig. 1(a)], where the properties of the entanglement transition have been most well established due to the ability to perform large-scale numerics. The model consists of a “brickwork” circuit of random two-site unitaries drawn uniformly from the Clifford group, operating on a linear chain of  $L$  qubits with periodic boundary conditions. In between each layer of unitaries, each site is measured in the  $Z$  basis with a fixed probability  $p$ . One tunes through the phase transition by changing  $p$ . Including the measurements, this random circuit is an example of a Clifford circuit, which, according to the Gottesman-Knill theorem, have the property that, for certain special initial states called stabilizer states, the action of the circuit can be simulated on a classical computer in a time that scales polynomially in  $L$  [30, 31]. As a result, one can perform a finite-size scaling analysis of the transition for hundreds or even thousands of qubits. Furthermore, polynomial-time classical algorithms have been introduced to compute entropies and mutual information of stabilizer states [32, 33]. Although these special properties of Clifford circuits make many aspects of their dynamics nongeneric, one of the defining features of the Clifford group is that it forms a unitary  $t$ -design for  $t \leq 3$  [34, 35]. This property implies that circuit-averaged properties of Clifford models often have similar phenomenology to more general quantum chaotic models [33, 36, 37]. The initial state can either be a mixed or pure stabilizer state, where a mixed stabilizer state is defined as the uniform mixture of all pure stabilizer states consistent with an incomplete set of stabilizers.

*Purification phases.*—The key signature of the purification transition is shown in Fig. 1(b). Here, we take  $L = 256$  and  $512$  sites and, starting from the completely-

mixed initial state,  $\rho = \mathbb{I}/2^L$ , we run many realizations of the random circuit out to a time  $t$  (= number of two-site unitaries that have acted on each qubit) that is a fixed multiple of  $L$ . We then compute the entropy density of the resulting state  $\langle S(\rho) \rangle / L$  averaged over random circuit realizations, assuming perfect knowledge of the outcome of all measurements in each run of the circuit [25–27]. For each such Clifford circuits started from this completely-mixed initial state, the von Neumann and all Renyi entropies are equal at a given time, although they differ between circuits and can decrease with time. Below a critical value of  $p = p_c = 0.1585(5)$  (determined to this level of precision below), we see that the late time density matrix has residual entropy density that is independent of  $L$  with the scaling  $\langle S(\rho) \rangle / L \sim (p_c - p)^\nu$  for  $\nu = 1.32(5)$ . On the other hand, for  $p > p_c$ , the average entropy density decays to zero with a decay rate that is independent of  $L$  (leading to a  $\sim \log L$  purification time). To the level of precision we can test, the values of  $p_c$  and  $\nu$  for the purification transition are identical to those for the entanglement phase transition for pure initial states. In this work, we will focus on the properties of the system near the critical point. Before describing those results, we first give some intuition for the physical origin of the two purification phases deep in their respective regimes.

The basic origin of the pure phase can be simply understood for  $p$  sufficiently close to one. In this limit, each layer of measurements projects the system into a near perfect product state in the  $Z$  basis. As a result, any correlations and complexity in the system can build up only over a few sites before being decohered by the measurements, which makes the system highly insensitive to initial conditions. Since pure states are a fixed manifold of the dynamics, the system will rapidly converge to zero entropy density, regardless of initial conditions.

The mixed phase generally has a richer many-body dynamics than the pure phase. It turns out some basic features of the mixed phase already appear when the measurements occur only at a single given site at an arbitrarily slow rate (technically, a sufficient condition for large  $L$  is  $p \ll 1/L^3$  [38]). In this limit, the spatial structure of the circuit is largely irrelevant for the late time dynamics, and we can replace the unitary between measurements by a random Clifford gate that acts on the entire set of  $L$  qubits. Starting from the completely-mixed initial state, the density matrix after the first measurement is

$$\rho_1 = \frac{1}{2^L} (\mathbb{I} + m_1 Z), \quad (1)$$

where  $m_1 = \pm 1$  is the first measurement outcome, and  $Z$  is the Pauli- $Z$  matrix on the site measured. The purity of the system has increased by a factor of 2. Following the intermediate time dynamics and second measurement, the density matrix is updated as

$$\rho_2 = \frac{P_2 U_2 \rho_1 U_2^\dagger P_2}{\text{Tr}[U_2^\dagger P_2 U_2 \rho_1]} = \frac{1}{2^L} (\mathbb{I} + m_2 Z + 2m_1 P_2 U_2 Z U_2^\dagger P_2), \quad (2)$$

where  $P_n = \frac{1}{2}(\mathbb{I} + m_n Z)$  is a projector onto the state consistent with the outcome of measurement  $n$  of  $m_n = \pm 1$  and  $U_n$  is the unitary for the random circuit between measurement  $n - 1$  and  $n$ . To compute the denominator of Eq. (2), we assume that  $U_2 Z U_2^\dagger \neq Z$  (this is true with probability  $1 - \frac{1}{4^{L-1}}$  since  $U_2$  maps  $Z$  to a random traceless product of Pauli operators on all  $L$  qubits), such that  $P_2 U_2 Z U_2^\dagger$  has zero trace. Using the property that the Clifford group is a 2-design, we can compute the circuit averaged purity after this second measurement

$$\langle \text{Tr}[\rho_2^2] \rangle = 3/2^L. \quad (3)$$

Extending these arguments to many subsequent measurements, one finds that, each time a measurement occurs, it increases the average purity by only  $1/2^L$  so

$$\langle \text{Tr}[\rho_n^2] \rangle = (n+1)/2^L, \quad n \ll 2^L, \quad (4)$$

leading to an exponentially long purification time. The average entropy satisfies the inequality

$$\langle S(\rho_n) \rangle \geq -\log_2 \langle \text{Tr}[\rho_n^2] \rangle = L - \log_2(n+1). \quad (5)$$

This limiting case establishes some essential features of the measurement-induced dynamics in the mixed phase. Although some aspects of the above argument extend to small but  $L$ -independent  $p$ , to establish the existence of the mixed phase in the present work, we rely on numerical solutions of the model. We now turn to an examination of the critical properties of the purification phase transition.

*Critical properties.*—One of the central findings of our study of this purification transition is that it occurs concurrently, and with the same critical exponents, as the entanglement phase transition for pure initial states. Thus, before examining the scaling behavior of the mixed state dynamics, we first revisit the critical properties of the entanglement phase transition for pure initial states. In Ref. [28], it was shown that the critical region of the entanglement phase transition can be precisely identified by looking at the mutual information  $I(A : B) = S(\rho_A) + S(\rho_B) - S(\rho_{A \cup B})$  between two antipodal regions on the circle of length  $L/8$  [see inset to Fig. 2(a)]. Here,  $\rho_c$  is the reduced density matrix on region  $C$ . Unlike the bipartite mutual information, which diverges logarithmically at the transition, this choice is convenient because this quantity vanishes on both sides of the transition with a finite peak at  $p = p_c$ . In Fig. 2(a), we show the finite-size scaling near the critical point for this antipodal mutual information starting from pure initial states. From collapsing the  $L = 128 - 512$  data we extract  $p_c = 0.1585(5)$  and  $\nu = 1.32(5)$ , which is consistent with the results reported in Ref. [28], with one digit of added precision on  $p_c$ .

Another basic quantity of interest in characterizing the transition is the correlation length  $\xi \propto |p - p_c|^{-\nu}$ . To realize a quantitative measure of the correlation length on

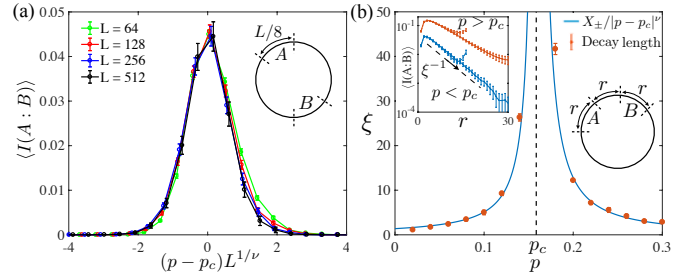


FIG. 2. (a) Antipodal mutual information for regions  $A$  and  $B$  of length  $L/8$  for pure initial states. The  $L = 64 - 256$  data were each slightly rescaled to have the same peak height as the  $L = 512$  data. Through a collapse of the  $L = 128 - 512$  data, we obtain  $p_c = 0.1585(5)$  and  $\nu = 1.32(5)$ . (b) Correlation length  $\xi$  extracted from the decay with  $r$  of  $I(A : B)$  for  $A$  and  $B$  of equal size  $r$  separated by a region of length  $r$ .  $\xi$  is well fit by the function  $X_\pm/|p - p_c|^\nu$  with  $X_\pm = 0.18/0.12$  for  $p \gtrless p_c$ . (inset) Sample of the data used to extract  $\xi$  for  $p \gtrless p_c$ ,  $L = 64$  and  $128$ , and  $t = 4L$ . Completely-mixed initial conditions were chosen to avoid a peak of order one that appears at  $r = L/4$  for pure initial states with  $p < p_c$ .

both sides of the transition, we study  $I(A : B)$  for the region shown in an inset of Fig. 2(b), where  $A$  and  $B$  are of equal size  $r$  and separated by a region of length  $r$ . The mutual information can be used to upper bound all connected correlation functions between  $A$  and  $B$  [39]. This quantity decays exponentially with  $r$  with a decay length that diverges as  $p \rightarrow p_c$ . To reliably extract the decay length we found that it is better to begin with the completely-mixed initial state because pure initial states for  $p < p_c$  develop a strong peak of order one at  $p = L/4$ , which obscures the exponential decay. This peak for pure initial states arises because of the volume-law entanglement, which implies that, when  $r = L/4$ ,  $I(A : B)$  begins growing linearly with  $r$  due to the volume-law scaling that appears for  $L/4 < r \leq L/3$ . Essentially,  $r \geq L/4$  is the regime where  $(A \cup B)^c$  is not larger than  $A \cup B$ , so it is an inadequate bath to fully decorrelate  $A$  and  $B$ . In contrast, for mixed initial states, the bipartite mutual information grows only logarithmically in time, leading to a weaker peak at  $r = L/4$  for early times.

With the basic, static scaling properties of the transition established, we can now turn to the dynamical scaling of the purification transition. The central results are summarized in Fig. 3, which shows the scaling behavior of the average entropy across the transition. Because of the apparent conformal symmetry at the critical point of this model [28], we assume a dynamical critical exponent  $z = 1$  and take a dimensionless scaling function for the entropy

$$\langle S(\rho) \rangle = F(x, \tau), \quad (6)$$

where  $x = (p - p_c)L^{1/\nu}$  and  $\tau = t/L$ . Note, that the scaling dimension of the entropy is zero, such that the

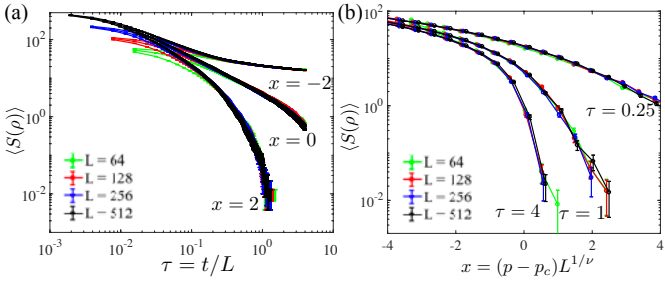


FIG. 3. (a) Average entropy  $\langle S(\rho) \rangle$  vs. scaled time  $\tau$  in the mixed phase  $p < p_c$ , at the critical point  $p = p_c$ , and in the pure phase  $p > p_c$ . (b) Finite-size scaling of  $\langle S(\rho) \rangle$  across the transition for different values of the scaled time.

$L$ -dependence of  $\langle S(\rho) \rangle$  enters only through the scaling function. This is consistent with the behavior we observed recently for a different class of open-system entanglement phase transitions [40]. In Fig. 3(a), we show the scaled time-dependence of the entropy across the phase transition. For  $p > p_c$ , there is rapid exponential decay of the entropy. At the critical point  $p = p_c$ , there is an intermediate time-scale over which we observe power law decay of the form  $F(0, \tau) \sim 1/\tau$ , which then crosses over to an exponential decay as the entropy approaches 1 bit. For  $p < p_c$ , we see an initially rapid decrease in the entropy, which crosses over towards an exponentially slow decay at late times. In Fig. 3(b), we plot the entropy across the phase transition for different values of the scaled time. In all cases, we see an excellent collapse of the data for  $L$  ranging from 64 to 512.

To make a more direct comparison between the purification phase transition observed for mixed initial conditions and the entanglement phase transition seen for pure initial states, it is natural to examine the bipartite mutual information  $I(A : A^c)$  for  $A$  of varying length  $r$ . For pure states,  $I(A : A^c)$  reduces to twice the entanglement entropy. The main qualitative features are illustrated in Fig. 4(a). For  $p \geq p_c$ , the mixed state purifies on a timescale at most linear in  $L$ , which implies that pure and mixed initial conditions have identical late-time scaling behavior for  $I(A : A^c)$ . In the pure or area-law phase, the long-time states exhibit only area-law mutual information, which quickly converges to a constant value independent of  $L$ . At the critical point, the system builds up logarithmic mutual information. The most significant result presented here is that, for  $p < p_c$ , we observe only a logarithmic scaling of  $I(A : A^c)$  for completely-mixed initial states in contrast to the volume-law scaling observed previously for pure-initial states. The presence of this logarithmic background for Clifford circuits was identified through an indirect measure in Refs. [27, 28]; however, we see here that the mixed state dynamics clearly reveals this feature by stripping away the volume-law entanglement of the pure state. Because of the exponen-

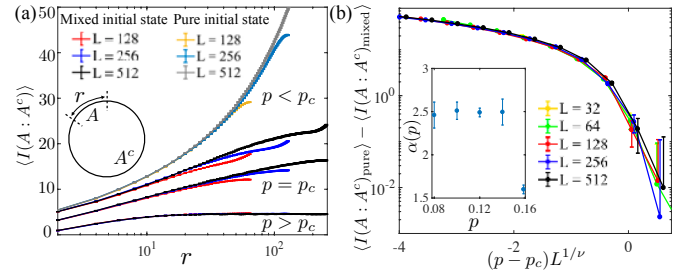


FIG. 4. (a) Finite-size scaling of the average bipartite mutual information  $\langle I(A : A^c) \rangle$  at  $t = 4L$  with  $A$  a contiguous region of length  $r$ , and  $A^c$  its complement. In the pure phase and at the critical point,  $\langle I(A : A^c) \rangle$  becomes independent of initial conditions, displaying area-law behavior in the pure phase and logarithmic scaling with  $r$  at the critical point. In the mixed phase,  $\langle I(A : A^c) \rangle$  strongly diverges between mixed and pure initial conditions, displaying volume-law scaling for pure initial states and logarithmic scaling for mixed states on this time scale. (b) Finite size-scaling of the difference of half-cut mutual information between pure and completely-mixed initial conditions at  $t = 4L$ . (inset) Coefficient of  $\log L$  contribution to halfcut mutual information (averaged over circuits and time  $2L < t < 6L$ ) for completely-mixed initial states.

tially slow purification, a weak signature of the volume-law entanglement of the pure state does appear as a small buildup of the bipartite mutual information near  $r = L/2$ .

Since the mixed state recovers the logarithmic contribution to the bipartite mutual information for  $p \leq p_c$ , a natural approach to finite-size scaling of the transition is to look at the difference of  $\langle I(A : A^c) \rangle$  between pure and completely-mixed initial conditions. The results are shown in Fig. 4(b), where we see an excellent scaling collapse of the data using the value of  $p_c$  and  $\nu$  obtained from Fig. 2(a). The presence of this logarithmic contribution to the mutual information for all  $0 < p < p_c$  is suggestive of critical behavior throughout the mixed phase. Writing  $\langle I(A : A^c) \rangle \sim 2\alpha(p) \log L$ , one signature of such behavior would be a nontrivial dependence of  $\alpha(p)$  on  $p$  away from the critical region  $\xi/L \gtrsim 1$ ; however, by computing the scaling of the halfcut bipartite mutual information with  $L$  in the mixed phase, we instead find that  $\alpha(p)$  is approximately constant and  $\approx 2.5(1)$  for  $p < p_c$  and  $\xi/L \ll 1$  [see inset to Fig. 4(b)]. At the critical point, where the system purifies after a time  $\sim L$ ,  $\alpha(p_c) \approx 1.63(3)$  [28].

*Conclusions.*—We have demonstrated the existence of a class of dynamical purification phase transitions between one phase where the many-body dynamics purifies arbitrary initial states at a rate independent of the system size, and another phase where the time to purify grows exponentially in the size of the system. We explored the scaling of the mutual information and of the dynamics associated with this phase transition. We studied a specific model of hybrid Clifford circuits that

is amenable to large scale numerics, however, the general features underlying the phase transition should be relevant for many physical systems undergoing high-fidelity, continuous monitoring, interspersed with entangling dynamics. Our observation that the bipartite mutual information grows only logarithmically in time for completely-mixed initial states should aid numerical studies of the transition in non-Clifford circuit models using matrix product methods. It appears from recent results, that the universality class of this phase transition differs between Clifford circuits and more general models [26, 28].

The perspective on the entanglement transition in terms of purification dynamics may also aid in experimental studies of the transition, where imperfections almost inevitably drive the system towards mixed states. As a concrete example, one can consider a type of local decoherence process where a  $Z$  measurement is made, but the result does not get recorded. Observing the volume-law entangled pure states at early times requires this local decoherence rate to scale as  $1/L^2$  or smaller. At long times, however, the density matrix will saturate to the type of mixed states studied in this work, unless the decoherence rate is exponentially small in  $L$ . In contrast, the purification transition will persist at long-times as soon as this local decoherence rate scales as  $1/L \log L$  or smaller.

Finally, we note that, the existence of the mixed phase, where the entropy density remains nonzero, implies that there is a “code space” of operators in the system that are not measured and, thus, can preserve quantum information about the initial state. In future work, it will be interesting to make a more direct connection between this property of the dynamics in the mixed phase and quantum error correcting codes.

We thank Ehud Altman, Soonwon Choi, Sebastian Diehl, Steve Flammia, Steve Girvin, Sarang Gopalakrishnan, Liang Jiang, Vedika Khemani, Andreas Ludwig, Adam Nahum, Jason Petta, Jed Pixley, Shivaji Sondhi and Justin Wilson for helpful discussions.

- 
- [1] M. A. Nielsen and I. L. Chuang, *Quantum Computation and Quantum Information* (Cambridge University Press, New York, NY, USA, 2011), 10th ed.
  - [2] J. I. Cirac, A. K. Ekert, and C. Macchiavello, *Optimal Purification of Single Qubits*, Phys. Rev. Lett. **82**, 4344 (1999).
  - [3] C. H. Bennett, G. Brassard, S. Popescu, B. Schumacher, J. A. Smolin, and W. K. Wootters, *Purification of noisy entanglement and faithful teleportation via noisy channels*, Phys. Rev. Lett. **76**, 722 (1996).
  - [4] L. J. Schulman and U. Vazirani, in Proceedings of the 31st STOC, edited by T. Leighton (ACM, New York, 1999), pp. 322 – 329.
  - [5] S. Bravyi and A. Kitaev, *Universal quantum computation with ideal Clifford gates and noisy ancillas*, Phys. Rev. A **71**, 022316 (2005).

- [6] F. Ticozzi and L. Viola, *Quantum resources for purification and cooling: fundamental limits and opportunities*, Sci. Rep. **4**, 5192 (2014).
- [7] L. Masanes and J. Oppenheim, *A general derivation and quantification of the third law of thermodynamics*, Nature Commun. **8**, 14538 (2017).
- [8] H. M. Wiseman and G. J. Milburn, *Quantum Measurement and Control* (Cambridge University Press, Cambridge, England, 2010).
- [9] P. Zoller, M. Marte, and D. F. Walls, *Quantum jumps in atomic systems*, Phys. Rev. A **35**, 198 (1987).
- [10] H. J. Carmichael, *An Open Systems Approach to Quantum Optics* (Springer-Verlag, Berlin, 1993).
- [11] M. B. Plenio and P. L. Knight, *The quantum-jump approach to dissipative dynamics in quantum optics*, Rev. Mod. Phys. **70**, 101 (1998).
- [12] A. R. Calderbank and P. W. Shor, *Good quantum error-correcting codes exist*, Phys. Rev. A **54**, 1098 (1996).
- [13] A. M. Steane, *Multiple-particle interference and quantum error correction*, Proc. R. Soc. Lond. A **452**, 2551 (1996).
- [14] J. Preskill, *Reliable quantum computers*, Proc. R. Soc. Lond. A **454**, 385 (1998).
- [15] D. B. Hume, T. Rosenband, and D. J. Wineland, *High-fidelity adaptive qubit detection through repetitive quantum nondemolition measurements*, Phys. Rev. Lett. **99**, 120502 (2007).
- [16] V. Negnevitsky, M. Marinelli, K. K. Mehta, H. Y. Lo, C. Flühmann, and J. P. Home, *Repeated multi-qubit readout and feedback with a mixed-species trapped-ion register*, Nature **563**, 527 (2018).
- [17] L. Jiang, J. S. Hodges, J. R. Maze, P. Maurer, J. M. Taylor, D. G. Cory, P. R. Hemmer, R. L. Walsworth, A. Yacoby, A. S. Zibrov, et al., *Repetitive Readout of a Single Electronic Spin via Quantum Logic with Nuclear Spin Ancillae*, Science **326**, 267 (2009).
- [18] P. Neumann, J. Beck, M. Steiner, F. Rempp, H. Fedder, P. R. Hemmer, J. Wrachtrup, and F. Jelezko, *Single-Shot Readout of a Single Nuclear Spin*, Science **329**, 542 (2010).
- [19] R. Vijay, D. H. Slichter, and I. Siddiqi, *Observation of quantum jumps in a superconducting artificial atom*, Phys. Rev. Lett. **106**, 110502 (2011).
- [20] G. de Lange, D. Ristè, M. J. Tiggelman, C. Eichler, L. Tornberg, G. Johansson, A. Wallraff, R. N. Schouten, and L. DiCarlo, *Reversing quantum trajectories with analog feedback*, Phys. Rev. Lett. **112**, 080501 (2014).
- [21] N. Ofek, A. Petrenko, R. Heeres, P. Reinhold, Z. Leghtas, B. Vlastakis, Y. Liu, L. Frunzio, S. M. Girvin, L. Jiang, et al., *Extending the lifetime of a quantum bit with error correction in superconducting circuits*, Nature **536**, 441 (2016).
- [22] Z. K. Minev, S. O. Mundhada, S. Shankar, P. Reinhold, R. Gutierrez-Jauregui, R. J. Schoelkopf, M. Mirrahimi, H. J. Carmichael, and M. H. Devoret, *To catch and reverse a quantum jump mid-flight*, arXiv:1803.00545 (2018).
- [23] X. Mi, M. Benito, S. Putz, D. M. Zajac, J. M. Taylor, G. Burkard, and J. R. Petta, *A coherent spin-photon interface in silicon*, Nature **555**, 599 (2018).
- [24] T. Nakajima, A. Noiri, J. Yoneda, M. R. Delbecq, P. Stano, T. Otsuka, K. Takeda, S. Amaha, G. Allison, K. Kawasaki, et al., *Quantum non-demolition measurement of an electron spin qubit*, Nature Nanotechnol. **396**,

- 1 (2019).
- [25] Y. Li, X. Chen, and M. P. A. Fisher, *Quantum zeno effect and the many-body entanglement transition*, Phys. Rev. B **98**, 205136 (2018).
  - [26] B. Skinner, J. Ruhman, and A. Nahum, *Measurement-Induced Phase Transitions in the Dynamics of Entanglement*, arXiv:1808.05953 (2018).
  - [27] A. Chan, R. M. Nandkishore, M. Pretko, and G. Smith, *Unitary-projective entanglement dynamics*, arXiv:1808.05949 (2018).
  - [28] Y. Li, X. Chen, and M. P. A. Fisher, *Measurement-driven entanglement transition in hybrid quantum circuits*, arXiv:1901.08092 (2019).
  - [29] S. Choi, Y. Bao, X.-L. Qi, and E. Altman, *Quantum error correction and entanglement phase transition in random unitary circuits with projective measurements*, arXiv:1903.05124 (2019).
  - [30] D. Gottesman, *The Heisenberg Representation of Quantum Computers*, arXiv:quant-ph/9807006 (1998).
  - [31] S. Aaronson and D. Gottesman, *Improved simulation of stabilizer circuits*, Phys. Rev. A **70**, 052328 (2004).
  - [32] K. M. R. Audenaert and M. B. Plenio, *Entanglement on mixed stabilizer states: normal forms and reduction procedures*, New J. Phys. **7**, 170 (2005).
  - [33] A. Nahum, J. Ruhman, S. Vijay, and J. Haah, *Quantum entanglement growth under random unitary dynamics*, Phys. Rev. X **7**, 031016 (2017).
  - [34] D. P. DiVincenzo, D. W. Leung, and B. M. Terhal, *Quantum data hiding*, IEEE Trans. Inform. Theory **48**, 580 (2002).
  - [35] Z. Webb, *The Clifford group forms a unitary 3-design*, Quantum Inf. Comput. **16**, 1379 (2016).
  - [36] A. Nahum, S. Vijay, and J. Haah, *Operator spreading in random unitary circuits*, Phys. Rev. X **8**, 021014 (2018).
  - [37] C. W. von Keyserlingk, T. Rakovszky, F. Pollmann, and S. L. Sondhi, *Operator hydrodynamics, otocs, and entanglement growth in systems without conservation laws*, Phys. Rev. X **8**, 021013 (2018).
  - [38] F. G. S. L. Brandao, A. W. Harrow, and M. Horodecki, *Local Random Quantum Circuits are Approximate Polynomial-Designs*, Commun. Math. Phys. **346**, 397 (2016).
  - [39] M. M. Wolf, F. Verstraete, M. B. Hastings, and J. I. Cirac, *Area laws in quantum systems: Mutual information and correlations*, Phys. Rev. Lett. **100**, 070502 (2008).
  - [40] M. J. Gullans and D. A. Huse, *Localization as an entanglement phase transition in boundary-driven Anderson models*, arXiv:1902.00025 (2019).